Proposal for the J-PARC 50 GeV Proton Synchrotron

Addendum to Direct measurement of the ${}^{3}_{\Lambda}$H and ${}^{4}_{\Lambda}$H lifetimes using the ^{3,4}He$(\pi^-, K^0)^{3,4}_{\Lambda}$H reactions

M. Agnello, S. Bufalino, G. Kaniadakis,
INFN - Sezione di Torino and
Politecnico di Torino, Department of Applied Science and Technology,
C.so Duca degli Abruzzi 24, 10129 Torino, Italy

E. Botta,
INFN - Sezione di Torino and University of Torino, Physics Department,
Via P. Giuria 1, 10125 Torino, Italy

T. Bressani, D. Calvo, A. Feliciello,
INFN - Sezione di Torino, Via P. Giuria 1, 10125 Torino, Italy

H. Tamura, Y. Ishikawa, A. Rogers,
Department of Physics, Tohoku University, Sendai 980-8578, Japan

T. Nagae,
Department of Physics, Kyoto University,
Kitashirakawa, Sakyo-ku, Kyoto, Japan

T. Takahashi, M. Ukai,
Institute of Particle and Nuclear Study (IPNS),
High Energy Accelerator Research Organization (KEK),
Oho 1-1, Tsukuba 305-0801, Japan

T.O. Yamamoto,
Advanced Science Research Center (ASRC),
Japan Atomic Energy Agency (JAEA),
Shirakata 2-4, Tokai, 319-1195, Japan

S. Ajimura, A. Sakaguchi,
Osaka University, Toyonaka, Osaka 560-0043, Japan

H. Outa
RIKEN, Wako, 351-0198, Japan

1 Introduction

We acknowledged the comments and remarks raised by the J-PARC Program Advisory Committee (PAC) and in this document we will try to answer to the different questions, as far as we understood them. We shall not treat here all the physics and instrumental aspects already described in the proposal. Instead, we will discuss in detail important items that perhaps were not (or not sufficiently) clear.

The central point is that the observable that we intend to measure is the lifetime of the hyperisotopes ${}^{3}_{\Lambda}\mathrm{H}$ and ${}^{4}_{\Lambda}\mathrm{H}$, that will be unavoidably affected by both statistical and systematic errors. The first one is essentially determined by the number of unambiguously observed events due to the mesonic decay of the hydrogen hyperisotopes, which in turn depends on the geometrical and instrumental features of the complexes of detectors and on the total amount of allocated beam time.

We estimated that 500 of such events should be enough for a determination of the lifetime at a satisfactory level. However, the systematic and, to some extent, the statistical errors depend on the cleanliness of the selected data sample. Such a feature is determined by the performances of the proposed complexes of detectors. In this respect, we do not understand the meaning of the wording "realistic (and proven) detector performances", since in our opinion we always quoted such numbers in the proposal. We will discuss this point in detail in the following, and we will show how different options for the realization of the detectors may affect the final precision of the measurement.

2 Realistic (and proven) detector performances

In our mind, the realistic performances of a complex of detectors are the ones reported in the international literature. Proven performances may be assumed as the ones actually achieved and published by members of the Collaboration. A side definition should be "available", which is not clearly settled at present, and on which several options should be anticipated. We will discuss these features in the following.

2.1 Intrinsic time resolution of the TOF array

Such a device does not exist and it should be assembled ex-novo. The START signal will be given by the beam scintillator(s) placed just in front of the re-

action target. The STOP signal will be provided by a cylindrical barrel of 20-30 slabs of scintillator (depending on the radius of the target's envelope). Similar arrangements were used in all the so far performed fixed target experiments aiming to determine the lifetime of Λ-hypernuclei. The pioneering experiment, performed about three decades ago [1] with a reduced solid angle of detection, reported an electronic time resolution of 92 ps (rms). A slightly better time resolution of 85 ps (rms) was achieved after about a decade in the series of experiments performed at a KEK PS with an increased solid angle of detection [2]. Few years before, some of us (proven experience) realized a scintillator barrel for the Time Of Flight system of the OBELIX Spectrometer at CERN [3], which was quite similar to that described in the present proposal. It consisted in 30 slabs of $80 \times 3 \times 1$ cm^3, each connected at both ends to Philips XP 2982 PMs through Lucite light guides, 80 cm long. Such an arrangement (10-stages PMs, long light guides) was due to the fact that the barrel was immersed into a magnetic field with B = 0.5 T and the PMs were hence installed in a quite far region with B = 0.01 T. A time resolution of 128 ps (rms) was obtained. In the P74 setup, the ∼30 cm long barrel will be located in a magnetic field free region and it will be equipped with 12-stages PMs, connected through short light guides. Therefore, an instrumental time resolution of 70-90 ps (rms) can be assumed, as stated in the proposal.

With the exception of the scintillators, all the necessary hardware (CFD discriminators, Mean Timer modules, 12-stages PMs) is already available.

2.2 Spatial resolution of the Drift Chambers

We remind that the drift chambers (DC) installed around the liquid He target in the P74 setup should accomplish two essential tasks: to measure the incidence angle on the range arrays (RA) of K^0_S and Λ-hypernucleus decay π^-s for their momentum determination and to allow the evaluation of the suited correction terms to the STOP - START time difference, described in details in Sec. 5. A spatial resolution of 100 μm (rms) for planar DC is a typical number obtained by many Groups or Collaborations in the last decades, exploiting different configurations of the electrodes or with different choices of the gas mixtures (see e.g. the excellent book [4]).

With regards to our proven experience on this item, some of us designed, constructed and finally operated for several years a set of 20 of such chambers in the FINUDA experiment. The measured spatial resolution over the full length of the drift cell, 5 cm wide, was better than 100 μm (rms); the gas mixture was (70%He, 30% iCH_4) [5, 6]. The 10 chambers of smaller dimensions (useful area 900×300 cm^2) could seem at first sight suited to the

new proposed experiment. However, they are not since the 100 μm spatial resolution along the drift cell gets much worse in the orthogonal direction (5 mm (rms)), as it was obtained by the charge division on the resistive anode wires. Such a configuration was optimized for the FINUDA experiment (DC immersed in a homogeneous solenoidal magnetic field). In the P74 experiment the same spatial resolution is mandatory for the two orthogonal coordinates. The coupling of two of such chambers, in order to obtain a good x-y resolution, appears unrealistic due to mechanical constraints.

We will investigate whether other members of the Collaboration have at disposal DC useful for the experiment or if it will necessary to build new ones.

2.3 Range Arrays

Complex RA composed by tens of scintillators of thicknesses varying from 2 to 4 mm, optimized for the detection of π^-s in the range 50-150 MeV/c were realized by members of the Collaboration in experiments with stopped K^- at the KEK PS [7] and afterwards with the SKS [2] (proven experience). The reported performances were very good, both for particle identification and energy resolution. Namely, for 100 MeV protons a resolution of $\sim$2 MeV was achieved [8]. The same result was previously reported by the experiment described in [9], in which one of the members of the P74 Collaboration was deeply involved. In addition, a resolution of $\sim$4.6 MeV (FWHM) was quoted for 100 MeV π^-s, corresponding to a momentum resolution of $\sim$2.4 MeV/c (rms) for $\sim$200 MeV/c π^-s. This is also confirmed by the only published kinetic energy distribution of $^{12}_{\Lambda}$C mesonic weak decay (MWD) π^-s [10], which has been obtained with the same range detector used in [2] for lifetime measurements. By taking into account the improvements in electronics and, in particular, in the photomultipliers performances, a resolution of 2 MeV/c (rms) seems to be realistic and achievable for π^- momenta in the range 70–140 MeV/c.

The energy of the π^- following both the K^0_S and the Λ-hypernucleus MWD and detected by the RA will be lower than 50 MeV. This fact ensures that the absorption of π^- before their stop will be of the order of 6-7%.

We are investigating how much of the existing hardware can be reused. In any case the final performances will be at the same level of the previous experiments or even better.

2.4 Beam line Spectrometer and SKS complex

The momentum resolution of the beam line spectrometer for the SKS at the KEK PS was 0.1% (FWHM), while the spatial resolution of the beam DC turned out to be 200-300 μm (rms) [7]. The expected resolution on the momentum of the K1.1 π^- beam is $\Delta p/p = 2 \times 10^{-3}$ (FWHM), while we assume that the spatial resolution of the chambers along the brand new beam line could be as good as 150 μm (rms).

The momentum of the scattered particles will be reconstructed by the SKS with the consolidated precision of $\Delta p/p = 2 \times 10^{-3}$ (FWHM) [11].

Members of the P74 Collaboration were engaged in these realizations and then they have a proven experience to achieve similar performances for the present experiment.

2.5 Liquid ^{3,4}He targets

There exist few liquid ^{3,4}He targets at J-PARC, used in previous experiments. We are investigating whether they could be available and, moreover, whether they can be adapted to the P74 experimental needs (see Sec. 4). In this respect, it is worth to remind that some members of the P74 Collaboration belong to the E13 Collaboration and they designed, build and successfully operated a liquid ^{4}He target [12].

3 Trigger strategy

We would like to point out that a very selective trigger strategy has been conceived to identify the events of interest and to reject the background. It is described in some details in the proposal; here we remind only that it is based on the detection of very asymmetric decays of the K^0_S produced together with the ${}^{3}_{\Lambda}$H/${}^{4}_{\Lambda}$H in the reaction

$$\pi^- + {}^{3,4}\mathrm{He} \rightarrow K^0 \ + \ {}^{3,4}_{\Lambda}\mathrm{H}. \qquad (1)$$

The π^+ is required to be emitted in the forward direction within a maximum angle with respect to the beam of 14° and with a momentum $\geqslant$ 600 MeV/c to match the SKS acceptance and to be detected with its best momentum resolution. Consequently, the π^- will be mostly emitted in the range 60°-110° with respect to the beam line and its momentum will be precisely measured by means of the DC and RA surrounding the target.

An appropriate selection will be applied to the difference between the crossing time of the π^- on the START scintillators and that of the K^0_S decay π^+ on the TOF wall downstream the SKS magnet.

To identify π^-s following K^0_S and Λ-hypernucleus decay, which have mostly a momentum $\leqslant$ 140 MeV/c, the signal from the last layer of each RA will be used in anticoincidence: π^-s with higher momenta, crossing the range without stopping, will be thus rejected to allow for a clean selection of events of interest.

As a last point, we remind that at the analysis level only the events in which a π^+ is detected in the SKS and two π^-s are detected in the DC and range module set will be used. For these events the K^0_S invariant mass will be reconstructed for the two possible (π^+,π^-) combinations and only if one of the two values will fall in an appropriate range centered on the Particle Data Group (PDG) K^0_S mass value [13] the event will be validated.

4 Monte Carlo simulations

Most of the conclusions drawn in the proposal and in this document are based on the outcome of a complete and detailed simulation program, developed in the framework of the Geant4 simulation toolkit [14] (see Fig. 1). Since the beginning of the experiment feasibility study, every sub-detector of the apparatus has been modeled through a careful description with a suitable level of detail. Particular attention has been put on the material budget in order to correctly account for the energy loss suffered by the particles following both the K^0_S and the Λ-hypernucleus decay.

This point is crucial for the accurate prong momentum determination by means of the range detector arrays (see Fig. 2). At present, the two vertical range modules measure 45 $\times$ 60 $\times$ 13.6 cm^3 and they consist of 34, 3 mm thick, scintillator layers (see Fig. 3). The two horizontal ones measure 75 $\times$ 60 $\times$ 13.6 cm^3 and also in this case each of them contains 34 scintillator layers. Each scintillator pad is enclosed in its own wrapping made of a thin aluminum mylar foil, 5 μm thick. The wrapped layers are interleaved by 1 mm of air.

The structure of the DC is made by a square 30 $\times$ 30 cm^2 (azimuthal chambers[1]) or 70 $\times$ 70 cm^2 (forward chambers[2]) aluminum frame, 5 cm wide (see Fig. 4). The 20 $\times$ 20 $\times$ 2 cm^3 and 60 $\times$ 60 $\times$ 2 cm^3 sensitive volumes are filled with a He (70%) + iC_4H_{10} (30%) gas mixture and they are enclosed by two mylar windows, 20 μm thick each.

In the present configuration the scintillator barrel for the time of flight measurement has a length of 30 cm (3 times the target length) and an internal radius of 10.5 cm. Each scintillator slab, 0.5 cm thick, is wrapped in a thin

[1] i.e. the 4 pairs of DC surrounding the target

[2] i.e. the pair of DC placed in front of the SKS

aluminum mylar foil, 5 μm thick. The barrel is coupled to a pair of beam scintillator arrays, whose overall dimensions 9.6 $\times$ 8.0 $\times$ 1.2 cm^3 were chosen on the basis of the know-how acquired by Collaborations who faced with similar experimental needs in the past (see Fig. 5).

As far as the liquid He target system is concerned, the current design was inspired by some examples found in literature (see Fig. 6). It was conceived by keeping in mind two key features. First, it should be long enough to guarantee an acceptable rate for the production reaction (1): its current length

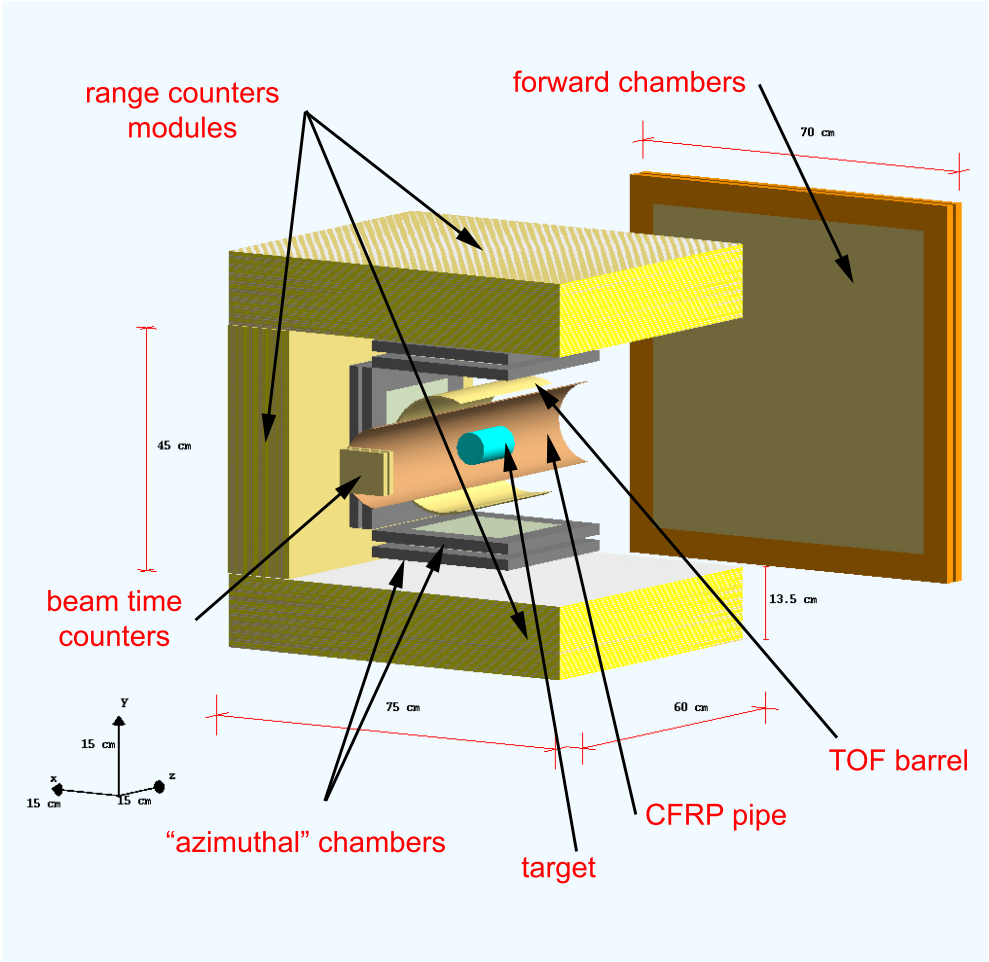

Figure 1: Pictorial view of the proposed *target-range hodoscope region* experimental set-up, as it is currently implemented in the GEANT4 simulation program. One of the quadrant of the apparatus has not been drawn to permit to see the interior details.

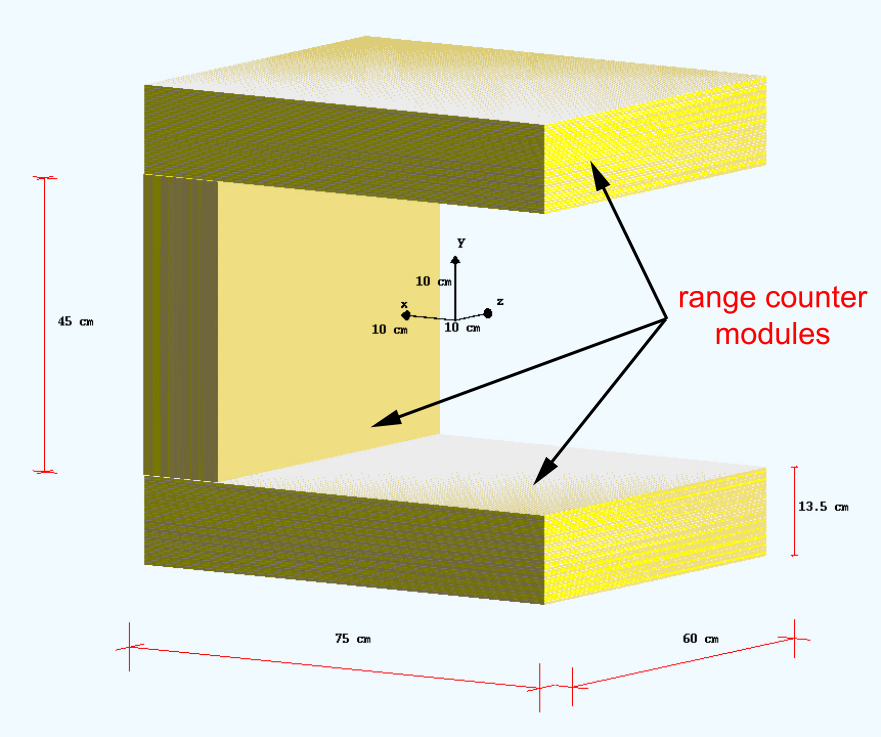

Figure 2: Pictorial view of the assembly of the range counter modules. One of the modules of the apparatus has not been drawn to permit to see the interior details.

is 10 cm. Second, it must be as "light" as possible in order to avoid that the momentum of particles following both the K^0_S and the Λ-hypernucleus decay will be degraded due to the crossing of unnecessary amount of dense material (liquid He). In the case of ^{3}He target this will imply also a reduced amount of the necessary, very expensive, raw material. For this reason, its radius is 3 cm only. In order to obtain the needed mechanical strength the cell is made by 800 μm aluminum cylinder. It is machined in such a way that two large 188 μm thick PET windows are present on the central upper and lower parts of the cell lateral surface, to minimize the multiple scattering effect on the particles emerging from the interaction vertex. Also the entrance and the exit windows are made by a 75 μm thick PET film. Finally, the target cell, kept under vacuum, is enclosed by a 600 μm thick CFRP pipe. Unlike the sub-detectors discussed above, the target assembly description includes also a simplified structure of the services, namely the piping for the He inlet and outlet. This way, the realistic effect due the multiple scattering suf-

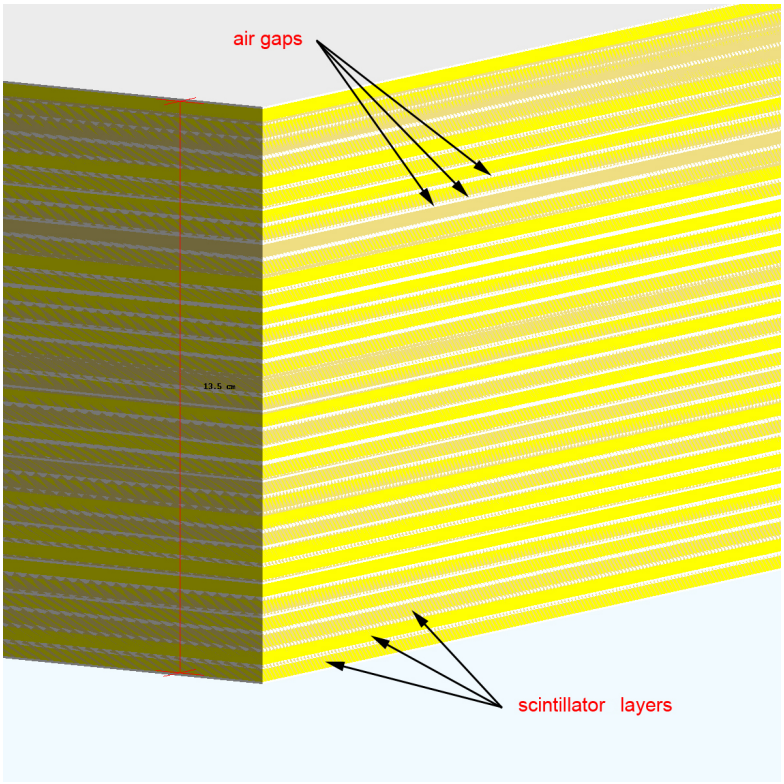

Figure 3: Magnified view of the cross section of a range counter module.

fered by the particles to be measured and the shadow effect on the detectors surrounding the target are properly taken into account.

5 Analysis of the time delay spectra and related errors

First of all we would like to underline that with our experimental approach the events in the time delay spectra useful for the analysis are not only those related to the two-body decays of the hydrogen hyperisotopes at rest, but also in flight. In addition, the three-body decays, both at rest and in flight, will be taken into account as well. We will not apply any selection on the momentum spectra of the decay π^-s, except a final consistency check in the ${}^{4}_{\Lambda}$H study, definitely easier than the ${}^{3}_{\Lambda}$H case. For this reason, from now on we will focus the attention on the ${}^{3}_{\Lambda}$H case only

Following the discussion of Sec. 2, we may assume a timing resolution

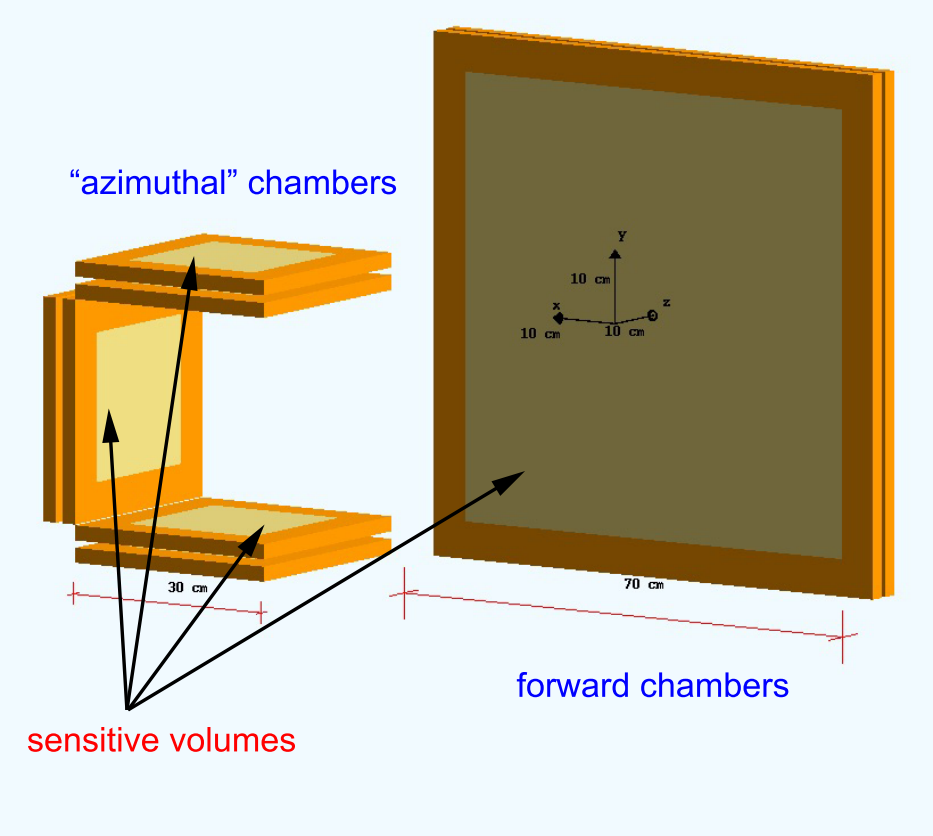

Figure 4: Pictorial view of the assembly of the azimuthal and the forward DC. One of the azimuthal chamber pairs has not been drawn to permit to see the interior details.

of 70-90 ps (rms), a beam spectrometer momentum resolution of 2×10^{-3} (FWHM), an SKS momentum resolution of 2×10^{-3} (FWHM) and a spatial precision of the beam DC of 150 μm (rms). Concerning the performances of the other ensembles of detectors (DC around the target, RA) they depend on the amount and on the quality of the devices that could be reused, not yet defined. Here we analyze their overall impact on the observable which has to be determined, the lifetime. In the following we will consider as realistic and achievable the values of 70-90 ps (rms) for the intrinsic time resolution of the TOF array and those reported above for the beam spectrometer and the SKS at the K1.1 installation at J-PARC. The performances of the planar DC and of the RA, for the detection of both the ${}^{3}_{\Lambda}$H/${}^{4}_{\Lambda}$H and the K^0_S decay products, will be considered at two levels: the first quoted in Sec. 2 (σ_{xy} = 100 mm and σ_p = 2 MeV/c), the second one downgraded by a factor of

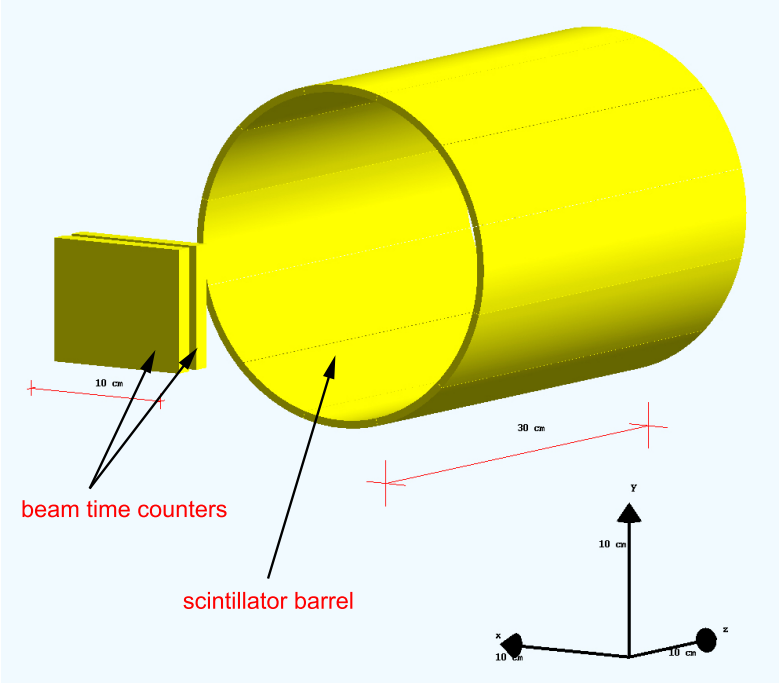

Figure 5: Pictorial view of the assembly of the time of flight system.

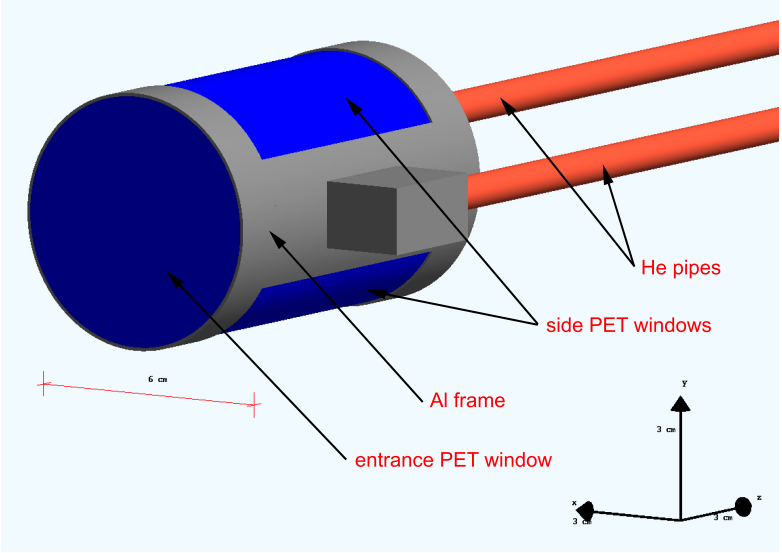

Figure 6: Pictorial view of the assembly of the liquid ^{3,4}He target.

2 and, respectively, of $\sqrt{2}$ with respect to the design performances, in the hypothesis of a possible reassembling of existing, not optimized, arrays of detectors.

We remind that the Λ-hypernucleus lifetime will be determined following the procedure sketched in Fig. 7. First, the time difference between the

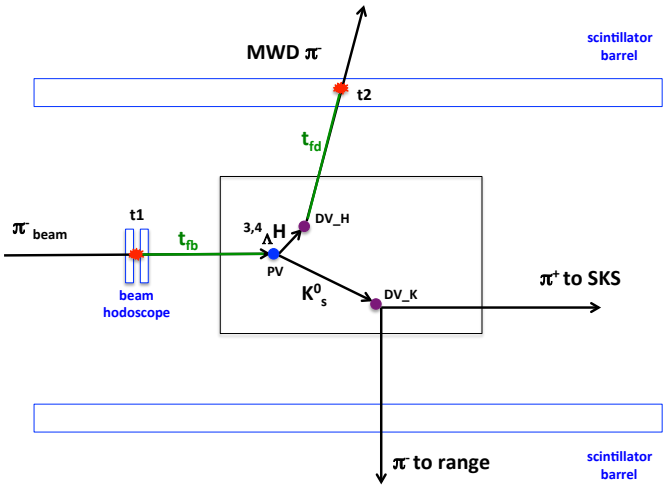

Figure 7: Scheme of the ${}^{3}_{\Lambda}\mathrm{H}/{}^{4}_{\Lambda}\mathrm{H}$ lifetime evaluation.

arrival times of the π^- from ${}^{3}_{\Lambda}\mathrm{H}/{}^{4}_{\Lambda}\mathrm{H}$ MWD on the scintillator barrel, t_2, and of the beam π^- on the beam timing hodoscope, t_1, will be measured. The two scintillator hodoscope elements should have been previously aligned in time and the resolution on the time difference should be ∼70-90 ps (rms) for each pair of slabs.

The time difference will be then corrected, event by event, to account for the beam flight time between the timing hodoscope and the production vertex PV (see Fig. 7), t_{fb}, and the weak decay π^- flight time between the Λ-hypernucleus decay vertex DV_H and the scintillator barrel slab, t_{fd}. The accuracy on the estimated correction terms, which anyway represent an essential step for the correct lifetime evaluation, crucially depends on the precision achieved in the localization of the three vertices. Actually, they are determined by an algorithm exploiting the position information on beam and decay π^-s, provided by the chambers along the beam line and surrounding the target, and the momentum information provided by the beam spectrometer, the SKS and the RA. Consequently, the global time

resolution on the lifetime determination turns out to be about 130 ps (rms), when one can firmly rely on the design performances. It worsens to 180 ps (rms) with a DC spatial resolution downgraded to 200 μm (rms).

The uncertainties on the localization capabilities of the decay DC and of the energy of the RA have a not negligible impact also on the number of events in the final time spectra. We may expect that such events should belong to two categories:

1. true events due to the decay of ${}^{3}_{\Lambda}$H (${}^{4}_{\Lambda}$H),

2. events due to the decay of quasi-free Λ.

We assume, as a minimal goal, that the spectra will contain 500 true events, as explained in the proposal. The estimated number of random coincidences should be negligible. The hardware trigger will be actually very selective and the effects due to a possible time structure of the extracted beam will be drastically reduced thanks to the replacement of the J-PARC main ring power supplies, already scheduled in the near future. In any case, the distribution of random coincidences over the full range of the lifetime interval examined (2 ns) should be fully flat.

The number of events due to quasi free Λ decays is large and it depends strongly on the resolution on the missing mass (MM) which will be attained. In turn, it depends on the resolution on the K^0_S invariant mass, determined by the design precision assumed for the DC and the RA. It is 3.5 MeV (rms) with the design performances, 3.9 MeV (rms) with the downgraded precision. The resolution on the ${}^{3}_{\Lambda}$H MM obtained is 2.0 MeV (rms) and 2.3 MeV (rms) for the two configurations. In the corresponding time spectra the amount of events due to quasi free Λ decays depends strongly on such a precision. In addition to the 500 events due to the ${}^{3}_{\Lambda}$H decay, we expect a consistent amount of events due to the quasi free Λ decay. The only experimental information on this subject may be inferred from the ${}^{3,4}_{\Lambda}$H MM spectra obtained in the ^{3,4}He$(e,e'K^+)^{3,4}_{\Lambda}$H reaction [15], shown by Fig. 8. Since in the Λ-hypernucleus production reactions $(e,e'K^+)$ and (π^-,K^0) the momentum transferred to the hyperon is almost the same, we may assume to a first approximation that the yield ratio of the ${}^{3}_{\Lambda}$H production and the quasi free continuum should be the same. For our purposes, we used the distribution shown by Fig. 9 in which the data collected at different angles in Ref. [15] were averaged taking into account also the angular acceptance of the SKS. For the time being, this distribution was obtained without considering the effect of the π^- absorption before their stop in the RA that in Subsection 2.3 we evaluated to be less than 6-7%.

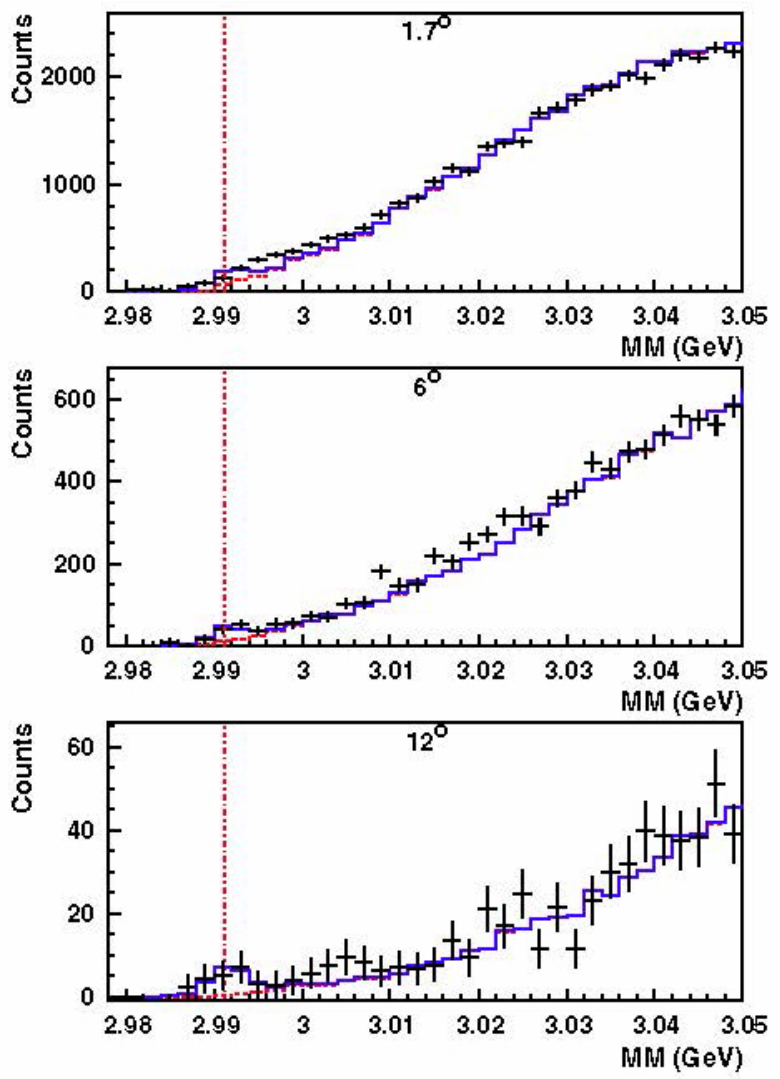

Figure 8: Reconstructed missing mass spectra for the ^{3}He$(e,e'K^+)^3_\Lambda$H reaction (from Ref. [15]).

The total time spectra will then be fitted taking into account the different contributions. For the signal and the Λ quasi-free ones, a convolution of the TOF system response function with a negative exponential will be used, with the known time resolution and Λ lifetime values, as already described in the P74 proposal. The fitting function will thus be:

$$S(t) \;=\; \int_0^\infty \left[\frac{1}{\tau_{hyp}} \exp^{-t'/\tau_{hyp}} \;+\; \left(\frac{S}{N}\right)^{-1} \; \frac{1}{\tau_\Lambda} \exp^{-t'/\tau_\Lambda} \right] R(t-t') \; dt' . \quad (2)$$

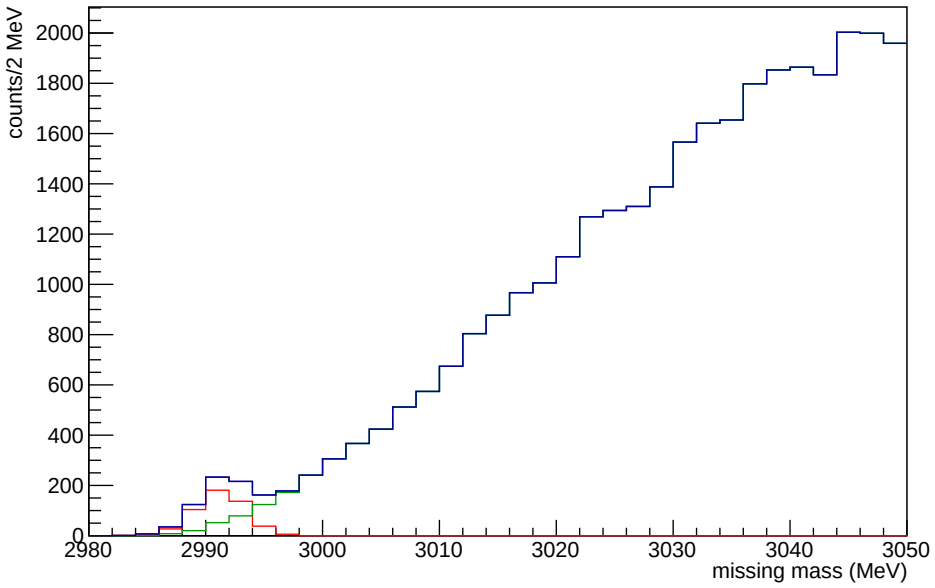

Figure 9: Reconstructed missing mass spectrum for the ^{3}He(π^-,K^0) reaction. The red histogram represents the signal from the $^3_\Lambda$H formation, the green one the quasi free contribution and the dark blue one the sum of the two components. See text for more details.

$R(t-t')$ is the detector response function, which in principle could be represented by any function in the fitting procedure. We recall that the precise shape of the $R(t-t')$ function will be obtained as explained in the proposal. At present we assume for it a Gaussian shape. When considering also a possible random coincidences contribution, a constant offset will be added to (2).

In the formula (2) there are three parameters, namely the free Λ and the Λ-hypernucleus lifetime and the S/N ratio. The Λ lifetime value could be either fixed to its PDG nominal value [13] or left to vary in the $(\tau_\Lambda - \sigma_{\tau_\Lambda}, \tau_\Lambda + \sigma_{\tau_\Lambda})$ interval, where σ_{τ_Λ} is the uncertainty reported by the PDG [13]. The S/N ratio could be extracted from a fit of the MM spectrum to a Gaussian, representing the signal, plus a polynomial, describing the background, performed over a range extending from the $^3_\Lambda$H mass nominal value minus two times the MM resolution up to, for example, the $^3_\Lambda$H mass nominal value plus 15-20 MeV. This way, the area of the Gaussian will give the S value, the area of the polynomial underneath the Gaussian will provide the N value. The obtained

S/N ratio will be allowed to vary according to the N statistics: for S = 500 and, let us suppose, N ≈ 400 the variability range would be ∼ ±5%. Finally the Λ-hypernucleus lifetime will be obtained from the convolution fit as free parameter.

The lifetime of ${}^{3}_{\Lambda}$H has been extracted in the above mentioned conditions of S/N and with the two hypotheses: $\tau({}^{3}_{\Lambda}\mathrm{H}) = 142$ ps and $\tau({}^{3}_{\Lambda}\mathrm{H}) = 242$ ps, corresponding to the lowest value published by the STAR Collaboration [16] and the highest one obtained by the ALICE Collaboration [17].

Fig. 10 shows a selected sub-sample of the outcome of the fit obtained with a global time resolution of 130 ps (rms). The χ^2 statistics is in every case $\leqslant 1$. As can be seen, both statistical and systematic errors amount each to ∼10% at maximum. Table 1 summarizes the expected precision and the accuracy values that should be achievable on the measurement of ${}^{3}_{\Lambda}$H lifetime when the apparatus design performances are effective. It has been checked

Table 1: Expected errors on the ${}^{3}_{\Lambda}$H lifetime determination as a function of different S/N ratio values, when the experimental apparatus features the design performances. The upper part of the table refers to the hypothesis of a short τ_{hyp}, while the lower part shows the results in the case of a τ_{hyp} very close to the lifetime of the free Λ.

simulated τ_{hyp} (ps)	guessed S/N	errors stat.	errors syst.
142	0.5	11%	3%
	1.0	10%	7%
	2.0	7%	6%
242	0.5	7.5%	5.4%
	1.0	7%	2%
	2.0	5%	10%

that when the flat random coincidences contribution is added the error remains practically unchanged. We can thus conclude that is reasonable to expect to be able to determine the ${}^{3}_{\Lambda}$H lifetime with a total error (statistical + systematic) $\leqslant$ 15% with the design performances of the apparatus components. We notice that the errors do not vary drastically as a function of the S/N ratio. Its actual value will be obviously determined from the experimental data. Fig. 11 shows a selected sub-sample of the outcome of the fit obtained with a global time resolution of 180 ps (rms). In table 2 we summa-

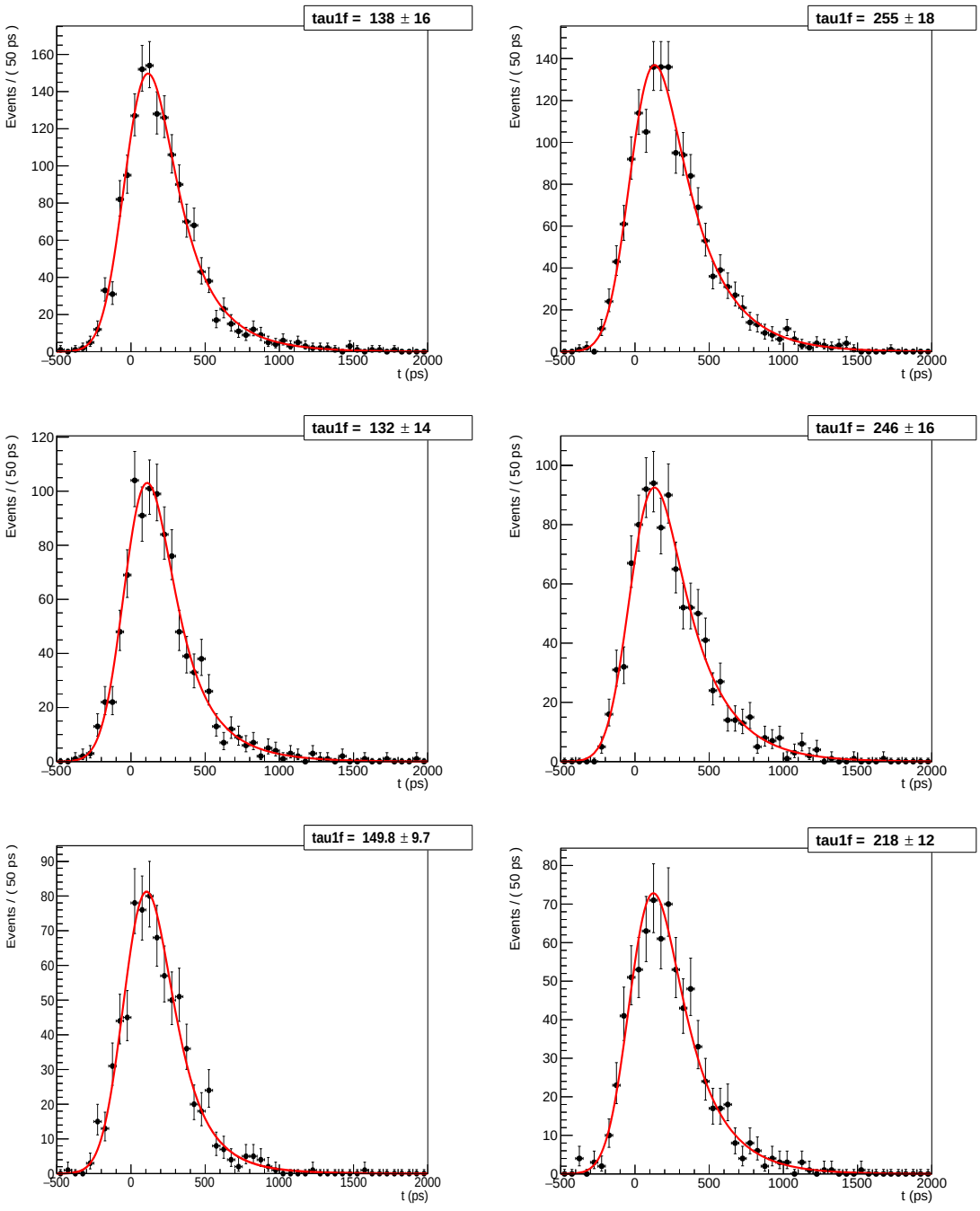

Figure 10: Fits to the corrected time distribution from signal and quasi-free Λ background according to the function (2), in the case of a global time resolution of 130 ps (rms). The plots on left column refer to a lifetime $\tau =$ 142 ps, while the ones on the right correspond to $\tau = 242$ ps. In both columns from top to bottom row the S/N ratio varies from 0.5 to 1 and finally to 2.

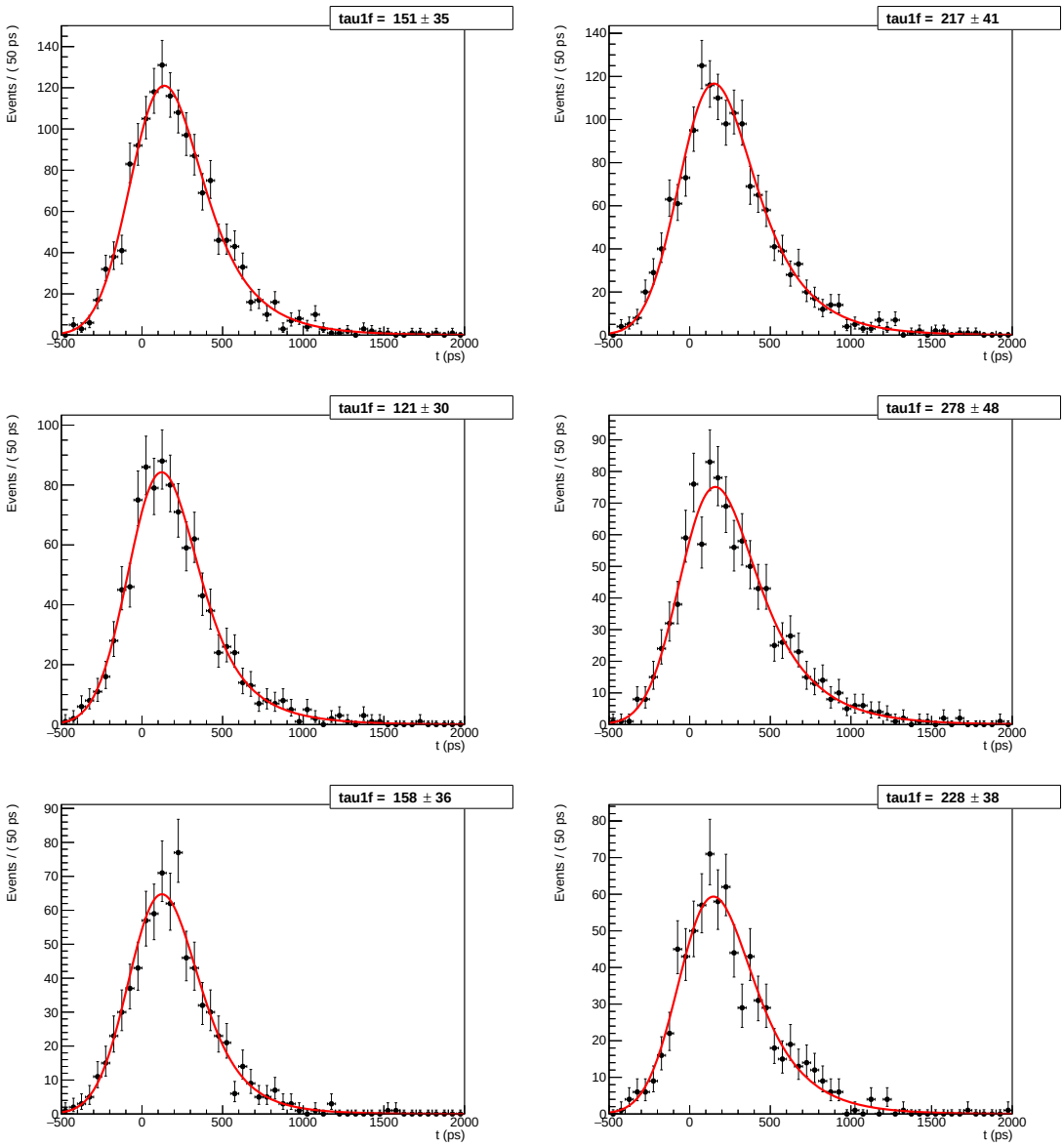

Figure 11: Fits to the corrected time distribution from signal and quasi-free Λ background according to the function (2), in the case of a global time resolution of 180 ps (rms). The plots on left column refer to a lifetime $\tau = 142$ ps, while the ones on the right correspond to $\tau = 242$ ps. In both columns from top to bottom row the S/N ratio varies from 0.5 to 1 and finally to 2.

rize the expected precision and the accuracy values that should be achievable on the measurement of ${}^{3}_{\Lambda}$H lifetime when one assumes a worsening by a factor of $\sim$2 of the experimental apparatus performances with respect the design ones. The negative impact on the lifetime extraction can be appreciated by comparing the results listed in Table 1 and Table 2.

Table 2: Expected errors on the ${}^{3}_{\Lambda}$H lifetime determination as a function of different S/N ratio values, when one assumes a significant worsening in the performance of the experimental apparatus with respect the design ones. The upper part of the table refers to the hypothesis of a short τ_{hyp}, while the lower part shows the results in the case of a τ_{hyp} very close to the lifetime of the free Λ.

simulated τ_{hyp} (ps)	guessed S/N	errors stat.	errors syst.
142	0.5	25%	6%
	1.0	21%	15%
	2.0	25%	11%
242	0.5	17%	10%
	1.0	20%	15%
	2.0	16%	6%

A final remark is that the π^- spectra corresponding to the 2- and 3-body ${}^{3}_{\Lambda}$H decays will be obtained at the same time (see Fig. 12). From these data it should be possible to determine the ratio of the two branching ratios with an error lower than the present one.

References

[1] J.J. Szymanski *et al.*, Phys. Rev. C 43 (1991) 849.

[2] H. Park *et al.*, Phys. Rev. C 61 (2000) 054004.

[3] G.C. Bonazzola *et al.*, Nucl. Instr. Meth. A 356 (1995) 270.

[4] W. Blum, W. Riegler, L. Rolandi in *Particle Detection with Drift Chambers* (Springer Verlag, Berlin, Heidelberg, 2008).

[5] M. Agnello *et al.*, Nucl. Instr. Meth. A 367 (1995) 100.

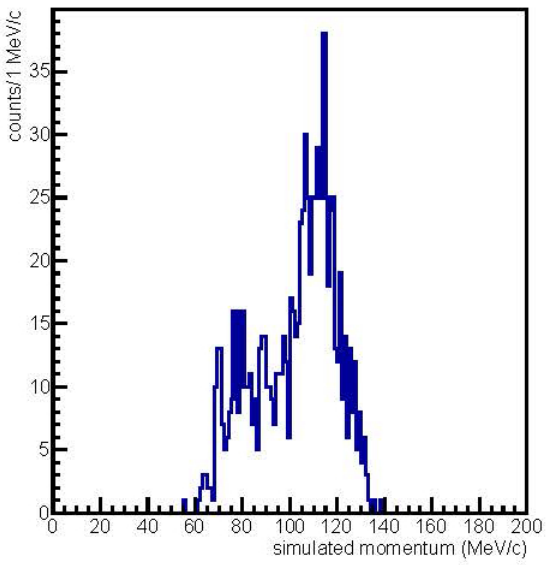

Figure 12: Simulated spectrum of the π^- from 2- and 3-body ${}^{3}_{\Lambda}\mathrm{H}$ decays as observed in the present experiment.

[6] E. Botta, PhD Thesis (1995).

[7] T. Fukuda *et al.*, Nucl. Instr. Meth. A 361 (1995) 485.

[8] H. Bhang *et al.*, Phys. Rev. Lett. 81 (1998) 4321.

[9] T. Bressani *et al.*, Nucl. Instr. Meth. 68 (1969) 13.

[10] Y. Sato *et al.*, Phys. Rev. C 71 (2005) 025203.

[11] T. Takahashi *et al.*, Prog. Theor. Exp. Phys. (2012) 02B010.

[12] T.O. Yamamoto *et al.* Phys. Rev. Lett. 115 (2015) 222501.

[13] M. Tanabashi *et al.* (Particle Data Group), Phys. Rev. D 98 (2018) 030001.

[14] GEANT4 Collaboration, Nucl. Instr. Meth. A 506 (2003) 250.

[15] F. Dohrmann *et al.*, Phys. Rev. Lett. 93 (2004) 242501.

[16] STAR Collaboration, Phys, Rev. C 97 (2018) 054909.

[17] ALICE Collaboration, Nucl. Phys. A **982** 815–818 (2019).